Structural, Morphological and Ferroelectric Properties of Dy doped 0.80$BiFeO_3$–0.20$PbTiO_3$ solid solution

Manoj Baloni
Department of Physics, SGRR (PG) College Dehradun,Uttarakhand, India

ABSTRACT

The solid state reaction technique was used to synthesize Dy modified $BiFeO_3$-$PbTiO_3$, i.e. 0.80$Bi_{1-x}Dy_xFeO_3$-0.20$PbTiO_3$ solid solution with x = 0.05 and 0.10 compositions. The rhombohedral to tetragonal phase transition of solid solutions was observed by the structural analysis based on X-ray diffraction (XRD) analysis. SEM micrographs revealed a dense microstructure with non-uniform grains, altering the ferroelectric characteristics of these solid solutions, and grain size decreases as Dy doping rises. Ferroelectric properties of the compounds are confirmed by electric field dependent polarization (PE-hysteresis) loops. The ability of samples for various electronics device applications may be related to ferroelectric loops with increased remnant polarization with increase in Dy doping.

Keywords: $PbTiO_3$, XRD, SEM, Ferroelectric Loops, Remnant polarization.
DOINumber:10.48047/nq.2022.20.22.NQ10384 **NeuroQuantology2022;20(22):3869-3876**

1. INTRODUCTION:

Multiferroics, which are materials with coupled ferroelectric, antiferromagnetic, and ferroelastic orderings, have piqued the interest of researchers. Multiferroics have received a lot of attention in recent years because of its prospective uses in electronic devices as well as their fascinating fundamental physics [1-3]. Ferroelectricity in multiferroic materials is produced by ions with a d^0 electronic state, and magnetism is produced by transition metal ions with d^n unpaired electrons. Researchers mainly concentrated on the magneto-electric materials helpful for devices in order to solve the d^0 vs. d^n challenge [4]. Researchers primarily concentrated on the magneto-electric materials helpful for devices in order to solve the d^0 vs. d^n challenge. It was discovered that $BiFeO_3$ (BFO) is one of these single-phase multiferroics with concurrent antiferromagnetic and ferroelectric order characteristics. Since the sources of ferroelectricity and antiferromagnetism are distinct and directly opposed, multiferroics like BFO have a weak interaction between them. Ferroelectric and anti-ferromagnetic transitions in BFO occur at transition temperature (T_C) 830°C and Neel temperature (T_N) 370°C, respectively [5-7].

BFO is a single-phase multiferroic compound that shows both ferroelectricity and G-type anti-ferromagnetism in its rhombohedral perovskite structure [8,9]. The magnetic spins of unpaired Fe^{3+} ions in BFO cause magnetism, whereas the displacement of Bi^{3+} ions from central-symmetric positions in regard to the oxygen ions around them produces ferroelectricity [10]. Due to suppressed linear magnetoelectric coupling caused by cycloidal spin modulation, BFO displays a very weak magnetoelectric coupling [11,12]. BFO also exhibits secondary phase development, low magnetization, high leakage current, poor

ferroelectric reliability, and high dielectric loss in addition to these shortcomings [13–15]. The occurrence of secondary phase development, which resulted in significant leakage current, was the reason of the poor ferroelectric behavior. Lattice site replacement in BFO with the suitable element/ion is determined to be the most efficient method among the numerous ways of enhancing the multiferroic characteristics of BFO [16,17]. It has already been proven that the substitution of rare earth ions at the Bi-site can enhance the magnetic, electrical, and magnetoelectric properties of BFO [18-20].

Room-temperature ferroelectric $PbTiO_3$ (PTO) with tetragonal symmetry (*P4mm*) and T_C = 490°C was added to BFO in order to increase thermal stability, decrease leakage, and increase volatility. Baloni et al. claimed in their analysis of the compounds' phase transition that the coexistence of two solid solutions with various symmetry may lead to an unstable morphotropic phase boundary (MPB) which is thought to have enhanced multiferroic characteristics [21]. Tetragonal and rhombohedral phases were found to coexist in BFO-PTO, as reported by Comyn et al [22]. According to Correas et al. [23], who discussed the potential phase transition in the compounds, the combination of these two solid solutions with different symmetry may result in MPBs, which are unstable martens tic phase boundaries between two phases that are thought to have increased piezoelectric and dielectric properties. It has been found that between 64% and 72% of BiFeO3 has the mixed phase area of the rhombohedral (R3c) and tetragonal (P4mm) symmetry, despite the fact that this region was thought to depend on the compositional process [24]. In ABO_3 type materials, the various B-site dopants (Al, Sc, In, Lu, Tm, Y, Gd, Sm, Nd, and La) have an impact on the bulk, grain boundary, stability, sinterability, lattice parameter, and total conductivity. According to Singh et al., $0.50(Bi_{1-x}La_xFeO_3)$-$0.50(PbTiO_3)$ exhibits better dielectric and magnetoelectric properties due to control over oxygen ion vacancy and ferroelectric transition temperature (T_C) by La substitution [25].

The Nd modified 0.7BFO-0.3PTO binary solid solution was investigated by N. Kumar et al., and found that the transition temperature decreased as Nd^{3+} ion concentration increased [26]. In 0.6BFO-0.4 PT, Dy^{3+} was substituted, which reduced the sample's conductivity [27]. The creation of composites including perovskite-type minerals, such as $BaTiO_3$, which enhance optical and multiferroic characteristics, has been covered in a number of literary works in recent years [28]. Other binary multiferroic perovskites were the subject of prior research into their structural, magnetic, piezoelectric, ferroelectric and optical properties, and it was found that the multiferroic properties had greatly improved [29]. As a result of the aforementioned factors, it is anticipated that the substitution of a rare earth element may result in increased ferroelectricity and lattice distortion, as well as contribute to fluctuation of oxygen ion vacancies that would help to offset the leakage current issue. In this investigation, $0.80Bi_{1-x}Dy_xFeO_3$-$0.20PbTiO_3$ with x = 0.05 and 0.10 were synthesized and their structural, morphological, and ferroelectric properties were examined.

2. EXPERIMENTAL DETAILS:

$0.80Bi_{1-x}Dy_xFeO_3$-$0.20PbTiO_3$ solid solution with x = 0.05 and x = 0.10 was synthesized using a solid state reaction approach. Analytical grade reagent powders of Bi_2O_3, Dy_2O_3, Fe_2O_3, PbO, and TiO_2 were weighed and thoroughly mixed in an agate mortar for four hours in acetone medium. A two-hour calcinations process at 820°C was performed on the finely ground powder. A 5% surplus of Bi_2O_3 was continuously added to the starting reactants during the synthesis to obstruct succeeding phases. The mixes were then processed for an additional two hours in the agate mortar after a few drops of a polyvinyl alcohol (PVA) binder were added to each powder composition. Pellet specimens with a 1 mm thickness and a 7 mm diameter were created by pressing blended powders of

various compositions into circular discs at a pressure of 1.5 x 08 Pascal. After that, the specimens were sintered at 840°C for two hours. On a Bruker D8 Advance X-ray diffractometer at room temperature, CuK radiation with a wavelength of 1.5406 Å was used to analyze the crystal structure of prepared samples. The surface morphology of synthesized materials was examined using a scanning electron microscope (Carl Zeiss EVO18) with 20KeV electron beam intensity. Shrunk, polishable pellets coated with high conducting silver paste were examined using a ferroelectric loop tracer (aiXACCT Systems GmbH aixPES) at room temperature to examine the polarization (P) vs electric field (E) loops.

3. RESULTS AND DISCUSSION:

The XRD pattern of $0.80Bi_{1-x}Dy_xFeO_3$-$0.20PbTiO_3$ solid solution with x = 0.05 and x = 0.10 in the 20°-60° range are shown in Figure 1. $BiFeO_3$ has rhombohedral crystal structure with the space group *R3c*, whereas $PbTiO_3$ has tetragonal symmetry with the space group *P4mm* [30,31]. It is observed that new peaks for 2θ, denoted as T in [Figure 1], arise at 21°, 23°, 50°, and 55° together with the XRD peaks corresponding to $BiFeO_3$ with increasing Dy doping. Tetragonal $PbTiO_3$ phase is responsible for these new peaks. It has been found that the face-centered cubic (fcc) structure with the distinct space groups *R3c* and *P4mm*, respectively, distinguishes between the rhombohedral and tetragonal phases. The fraction of *R3c* phase, however, drops when Dy concentration rises from x = 0.05 to 0.10, whereas the fraction of *P4mm* phase rises. Additionally, such substantial changes in the XRD pattern imply that the Dy dopant substituted at the Bi site of BFO aids in suppressing the sharp diffraction peaks associated with BFO phase in the doped samples in order to produce improved $PbTiO_3$ phase.

The lattice parameters of prepared samples corresponding to rhombohedral structure (equivalent hexagonal), where miller indices (hkl) of the two highest intensity peaks of the XRD pattern, namely (012) and (110) are taken, and tetragonal structure, where miller indices (hkl) of the two highest intensity peaks of the XRD pattern, namely (100) and (001) are taken, are shown in Table 1. The interplaner spacing (*d*) is obtained by the equation $2d\sin\vartheta=n\lambda$, where *n* is the number of interplaner spacing and λ is the x-ray wavelength (1.5406Å). The lattice parameters for tetragonal and rhombohedral structures are shown in Table 1. It is abundantly obvious from the variations in lattice characteristics that the Bi^{3+} site is significantly impacted by Dy^{3+} intrusion. Earlier study on BT-PT binary systems doped with rare earth elements revealed similar results [32,33].

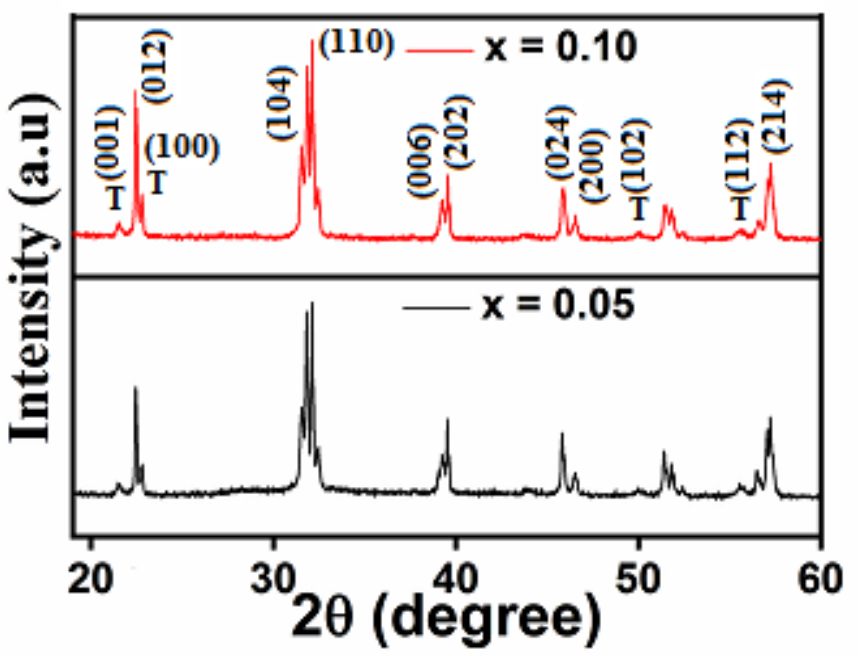

Figure 1. X-ray diffraction spectra of 0.80$Bi_{1-x}Dy_xFeO_3$-0.20$PbTiO_3$ solid solution with *x* = 0.05 and *x* = 0.10 compositions.

Table 1.
Lattice Parameters and Average Grain size of 0.80$Bi_{1-x}Dy_xFeO_3$-0.20$PbTiO_3$ solid solution with *x* = 0.05 and *x* = 0.10 compositions.

Composition *x*	Crystal Structure	Lattice Parameters	Average Grain Size (μm)
0.05	Rhombohedral (*R3c*)	a =5.5567Å b =5.5567Å c =13.45 Å	1.63
	Tetragonal (*P4mm*)	a = 3.8825 Å b = 3.8825 Å c =4.1037 Å	
0.10	Rhombohedral (*R3c*)	a =5.5503Å b =5.5503Å c =13.10 Å	1.30
	Tetragonal (*P4mm*)	a = 3.8793 Å b = 3.8793 Å c =4.1004 Å	

Morphological Studies: Surface morphology of 0.80$Bi_{1-x}Dy_xFeO_3$-0.20$PbTiO_3$ solid solution with *x* = 0.05 and *x* = 0.10 compositions is shown in Figure 2. The grain size data of solid solutions are shown in Table 1. All the ceramics exhibit dense microstructure without any pores and

contained well-developed grains. The diagram shows that the grain size of solid solutions reduces steadily with Dy content, from 1.63µm to 1.30 µm. Similar phenomena have been reported in prior investigations [34, 35]. This could be explained by the random distribution of Bi^{3+} and Dy^{3+} in the crystal lattice, which obliterates the internal structure and restricts grain formation. Further evidence that the doped Dy ions have successfully entered the lattice is provided by the fact that every component of the compound is dispersed quite equally. Additionally, oxygen vacancy levels and ion transport rates have an impact on grain formation [36]. Pure $BiFeO_3$ has a significant amount of oxygen vacancies due to the high volatility of Bi. Dy has a higher valence than Fe, which lowers the creation of oxygen vacancies and, in turn, reduces the average particle size.

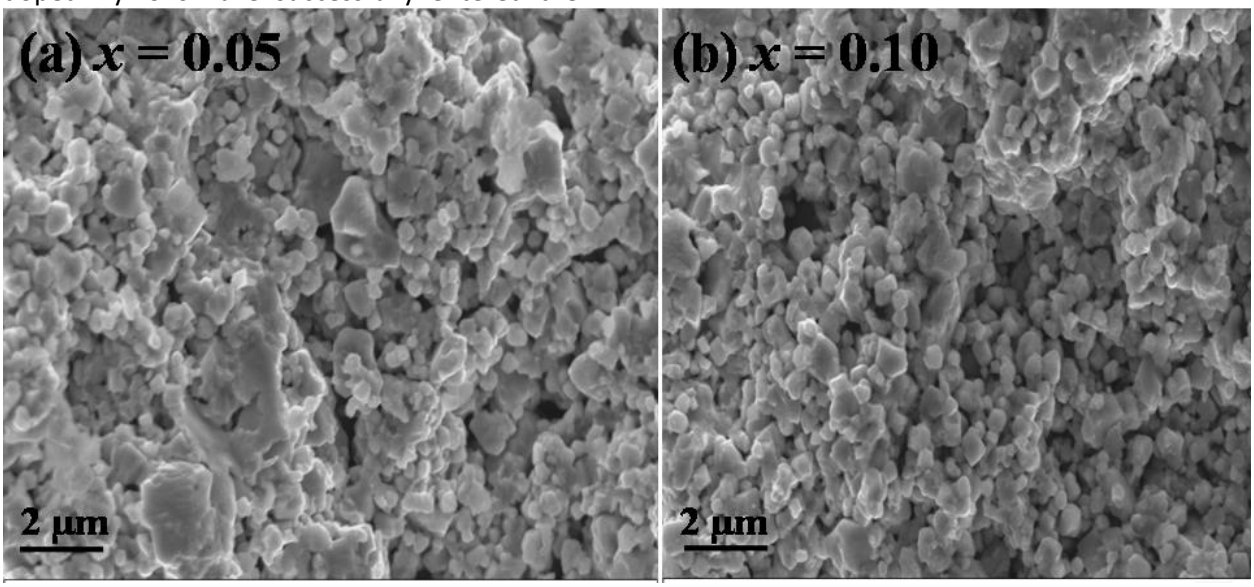

Figure 2. SEM images of $0.80Bi_{1-x}Dy_xFeO_3$-$0.20PbTiO_3$ solid solutions with x = 0.05 and x = 0.10 compositions.

Figure 3. display room temperature polarization versus electrical field (PE) loops for the purpose of further analyzing the impact of the aforementioned state of chemical homogeneity on ferroelectric characteristics. All ceramic loops are seen to not be saturated due to the minimal electrical field that is applied in order to prevent sample breakage. However, chemically homogeneous Dy substituted 0.80BFO-0.20PTO ceramics nonetheless exhibit improved remnant polarization. It is commonly accepted that the enhanced ferroelectric characteristics are significantly influenced by the better electric insulation in doped $BiFeO_3$ systems [37]. Additionally, for prepared solid solutions, the rise in residual polarisation is seen, which may be the result of the higher hybridization of Bi^{3+} and O^{2-} due to the shortening of the Bi-O bond length. This outcome is similar with the earlier findings [38]. For x = 0.05 and 0.10, the observed remnant polarization (P_r) is found to be 0.2562 and 0.5280 µC/cm^2, with coercive fields of 9.8307 and 16.7360 kV/cm, respectively.

However, the remnant polarization and coercivety of the Dy doped BFO-PTO samples are increased with increasing Dy doping. Nevertheless, the prepared samples are found to be a little lossy because the loop of the samples covers a larger region. This might be as a result of the Fe-site Dy substitution compensating for the oxygen ion vacancy. Sample energy dissipation is represented by the area underneath the loops. The performance of the sample's energy storage can be related to

eISSN1303-5150

its ferroelectric behavior, as reported by Xu et al. [39].

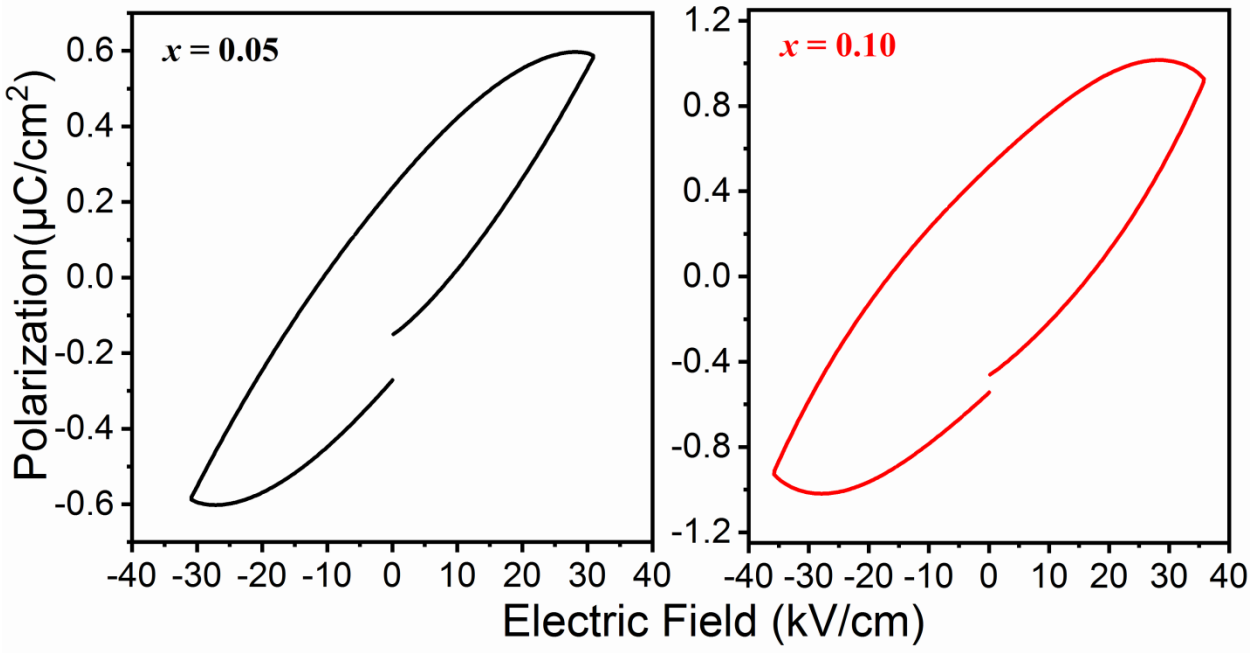

Figure 3. Ferroelectric hysteresis loops (P-E loops) of $0.80Bi_{1-x}Dy_xFeO_3$-0.20$PbTiO_3$ solid solutions with x = 0.05 and x = 0.10 compositions.

CONCLUSIONS:

The traditional solid-state reaction method was successfully used to synthesize $0.80Bi_{1-x}Dy_xFeO_3$-0.20$PbTiO_3$ solid solutions for x = 0.05 and x = 0.10 compositions. In addition to a rhombohedral crystal structure with the *R3c* space group, XRD analysis shows a tetragonal (*P4mm*) crystal structure with increasing Dy doping. Morphological studies show that the produced materials' grain sizes have been reduced from 1.63 µm to 1.30 µm. Lattice parameter reduction demonstrates unequivocally that Dy doping significantly affects structural characteristics. The produced compound is shown to be less lossy despite having higher residual polarization and coercivity. It will be accurate to say that the Dy substitution lead to materials with a low concentration of oxygen vacancies and a high capacity for energy storage.

REFERENCES

1. H. Béa, M. Gajek, M. Bibes and A. Barthélémy, Spintronics with multiferroics, J. Phys. Condens. Matter 20 (2008) 434221-1-11.
2. Y.-H. Chu et al., Electric-field control of local ferromagnetism using a magnetoelectric Multiferroic, Nature Mater. 7 (2008) 478–482.
3. P. Rovillain et al., Electric-field control of spin waves at room temperature in multiferroic $BiFeO_3$. Nature Mater.9 (2010) 975–979.
4. K. Auromun , S. Hajra, R.N.P. Choudhary and B. Behera, Structural, dielectric and electrical characteristics of yttrium modified 0.7$BiFeO_3$-0.3$PbTiO_3$, Solid State Sciences 101 (2020) 106139.
5. Z.X. Cheng et al., Enhancement of ferroelectricity and ferromagnetism in rare earth element doped BiFeO3, J. Appl. Phys.104 (2008),116109- 1- 116109-3.
6. A. Kornev and L. Bellaiche, Nature of the ferroelectric phase transition in multi

ferroic $BiFeO_3$ from first principles, Phys. Rev. B 79 (2009) 100105 (R).
7. R. Haumont et al., Phase stability and structural temperature dependence in powdered multiferroic $BiFeO_3$, Phys. Rev. B 78 (2008) 134108.
8. M. Cebela, D. Zagorac, K. Batalovic, J. Radakovic, B. Stojadinovic, V. Spasojevic and R. Hercigonja, BiFeO3 Perovskites: A multidisciplinary approach to multiferroics, Ceram. Int. 43 (2017) 1256-1264.
9. M. K. Singh, R. S. Katiyar, W. Prellier, and J. F. Scott, The Almeida–Thouless line in $BiFeO_3$: is bismuth ferrite a mean field spin glass, J. Phys.: Condens. Matter 21 (2009) 042202.
10. G. Catalan and J. F. Scott, Physics and applications of bismuth ferrite, Adv. Mater. 21 (2009) 2463 –2485.
11. C. T. Munoz, J. P. Rivera, A. Monnier, and H. Schmid, Measurement of the Quadratic Magnetoelectric Effect on Single Crystalline $BiFeO_3$, Japanese J. of Appl. Phys. 24 (1985) 1051-1053.
12. S. V. Surynarayana, Magnetoelectric interaction phenomena in materials, Bull. Mater. Sci.17 (1994) 1259-1270.
13. L.-F. Zhu et.al., Enhanced piezoelectric properties of $Bi(Mg_{1/2}Ti_{1/2})O_3$ modified $BiFeO_3$ –$BaTiO_3$ ceramics near the morphotropic phase boundary, J. Alloy. Comp. 664 (2016) 602–608.
14. Q. Li, J. Wei, J. Cheng and J. Chen, High temperature dielectric, ferroelectric and piezo- electric properties of Mn-modified $BiFeO_3$-$BaTiO_3$ lead-free ceramics, J. Mater. Sci. 52 (2017) 229–237.
15. X.X. Shi, X.Q. Liu and X.M. Chen, Readdressing of magnetoelectric effect in bulk $BiFeO_3$, Adv. Funct. Mater. 27 (2017) 1604037.
16. D.P. Dutta et al., Magnetic, ferroelectric, and magneto capacitive properties of sono-chemically synthe- sized Sc-doped BiFeO3 nano particles, J. Phys. Chem. C 117 (2013) 2382.
17. D.P. Dutta et al., Improved magnetic and ferroelectric properties of Scand Ti co doped multiferroic nano BiFeO3 prepared via sono-chemical synthesis, Dalton Trans. 43 (2014) 7838.
18. S.R. Das, R.N.P. Choudhary, P. Bhattacharya and R.S. Katiyar, Structural and multiferroic properties of La-modified $BiFeO_3$ ceramics, J. Appl. Phys. 101 (2007) 034104-7.
19. K. Chakrabarti et.al. Enhanced magnetic and dielectric properties of Eu and Co co-doped $BiFeO_3$ nano-particles, Appl. Phys. Lett. 101 (2012) 042401-3.
20. V.A. Khomchenko et.al., Crystal structure and multiferroic properties of Gd-substituted $BiFeO_3$, Appl. Phys. Lett. 93 (2008) 262905-3.
21. M. Baloni et al., Structural modification and evaluation of dielectric, magnetic and ferroelectric properties of Nd- modified $BiFeO_3$ – $PbTiO_3$ multiferroic ceramics, Ferroeletric 589 (2022) 161-176.
22. T. P. Comyn et.al., High temperature neutron diffraction studies of $0.9BiFeO_3$-$0.1Pb\ TiO_3$, J. Appl. Phys. 105 (9) (2009), 094108.
23. C. Correas, T. Hungría and A. Castro, Mechanosynthesis of the whole $x$$BiFeO_3$–(1-$x$) $PbTiO_3$ multiferroic system: structural characterization and study of phase transitions, J. Mater. Chem. 21 (2011) 3125–3132.
24. W.-M. Zhu et ai., Structure and properties of multiferroic (1- x) $BiFeO_3$– $x$$PbTiO_3$ single crystals, J. Mater. Res. 22 (8) (2007) 2136–2143.
25. A. Singh, A. Gupta and R. Chatterjee, Enhanced magnetoelectric coefficient (α) in the modified BiFeO3–PbTiO3 system with large La substitution, Appl. Phys. Lett. 93 (2008), 022902.
26. N. Kumar, B. Narayan, M. Kumar, A.K. Singh, S. Dhiman, S. Kumar, Effect of Nd^{3+} substitution on structural, ferroelectric, magnetic and electrical properties of $BiFeO_3$– $PbTiO_3$ binary system, SN Appl. Sci. 1 (8) (2019) 874.

eISSN1303-5150

27. N. Kumar, S. Kumar, B. Narayan, S. Bansal, A.K. Singh, Effect of Dy^{3+} substitution on structural, magnetic and dielectric properties of BiFeO3-PbTiO3 multiferroics, 1- 4, 13th Nanotechnol. Mater. Dev.Conf.(NMDC) 1 (8) (2019), 874.
28. M.Shariq, D. Kaur and V.C. Chandel, Structural, magnetic and optical properties of mulitiferroic $(BiFeO3)_{1-x}$ $(BaTiO3)_x$ solid solutions. Chin. J. Phys. 55 (2017) 2192–2198.
29. Z. Yao et.al., Structure and electrical properties of ternary $BiFeO_3$ -$BaTiO_3$-$PbTiO_3$ high-temperature piezo ceramics, J. Adv. Cream.1 (2012) 227-231.
30. S. Kumar et al., Correlation between multiferroic properties and processing parameters in $NdFeO_3$–$PbTiO_3$ solid solutions, J. Alloys. Compd. 764 (2018) 824–833.
31. T. Sahu, and B. Behera, Investigation on structural, dielectric and ferroelectric properties of samarium-substituted $BiFeO_3$–$PbTiO_3$ composites, J. Adv. Dielectr. 7 (2017) 1750001.
32. M. Baloni et al., Effect of Nd doping on structural, dielectric, magnetic and ferro-electric properties of $0.8BiFeO_3$-0.2Pb TiO_3 solid solution, J. Alloys Compd. 905 (2022) 164228.
33. J. Cheng, N. Li and L. E. Cross, structural and dielectric properties of Ga-modified $BiFeO_3$-$PbTiO_3$ crystalline solution, J. Appl. Phys. 94 (2003) 5153-5157.
34. D. Wang et al., Bismuth ferrite-based lead-free ceramics and multilayers with high recoverable energy density, J. Mater. Chem. A. 6 (2018) 4133–4144.
35. X. Wang et al.,Characteristics of giant piezoelectricity around the rhombohedral-tetragonal phaseboundary in (K,Na)NbO3-based ceramics with different additives, J.Mater. Chem.A. 3 (2015) 15951–15961.
36. A. Brinkman et al., Magnetic effects at the interface between non-magnetic oxides, Nat. Mater. 6 (2007) 6493–496.
37. S. Huang, Q. Li, L. Yang, J. Xu, C. Zhou, G. Chen, C. Yuan, G. Rao, Enhanced piezo-electric properties by reducing leakage current in Co modified $0.7BiFeO_3$-$0.3BaTiO_3$, Ceram. Int. 44 (2018) 8955–8962.
38. N. Wang et al., Investigation of structural, ferroelectric and magnetic properties of Ca modified $BiFeO_3$–$BaTiO_3$ ceramics, Ceram. Int. 46 (2020) 3855–3860.
39. M. Xu et al., Enhanced energy storage performance of (1-*x*)(BCT-BMT)-*x*BFO lead-free relax or ferroelectric ceramics in a broad temperature range, J. Alloys Compd. 789 (2019) 303–312.